Analysis of Retaining Structures With Skew Reinforcement

S. Bang and H. Yeon

A method of analyzing earth-retaining structures with skew reinforcement based on the principle of generalized plane-strain finite-element analysis is presented and it can calculate quasi-three-dimensional responses of the soil and the structural elements without resorting to a fully three-dimensional finite-element analysis. A significant reduction in computational effort with little loss in accuracy has been obtained. The developed method of analysis has been applied to investigate the effect of reinforcement skew angle associated with the Reinforced Earth retaining wall and the conventional tie-back concrete retaining wall.

Many earth-retaining structures use some kind of reinforcing technique to increase stability, including the Reinforced Earth wall (1), the Retained Earth wall (2), soil nailing (3), anchored bulkhead, and conventional retaining wall with tie-backs. All those methods use internal reinforced members installed within the backfill. However, a deviation from the standard method of construction is sometimes inevitable when those structures are used as bridge abutments. For instance, many bridge abutments are skew (i.e., the abutments are not perpendicular to the alignment of the bridge owing to the constraint imposed by the geometric conditions). Therefore, it is necessary under such circumstances to use skew-reinforcing members so that adequate friction develops along the length of the reinforcement or sufficient passive resistance develops in front of the deadman.

A truly three-dimensional analysis may have to be performed to analyze such skew retaining structures. However, if the reinforcements are parallel with one another and have the same geometric and material properties, then the analysis can be simplified to quasi-three dimensional (4). This paper summarizes one method and illustrates how the method can be applied to analyze earth-retaining structures with skew reinforcement.

METHOD OF ANALYSIS

The detailed behavior of the soil, the retaining structure, and the reinforcement must be taken into account in formulating a method of analysis. Those factors that greatly influence the performance of the earth-retaining structures generally favor the use of the finite-element method of analysis.

A generalized plane-strain condition (5) has been assumed to study the behavior of earth-retaining structures with skew reinforcement. The generalized plane-strain approach simply

Department of Civil Engineering, South Dakota School of Mines and Technology, Rapid City, S. Dak. 57701.

dictates that the plane-strain directional strain ε_z remains zero instead of the plane-strain directional displacement w being zero, as is commonly adopted in the conventional plane-strain approach. Therefore, the approach includes three nonzero displacement components u, v, and w along the x, y, and z coordinates, none of which is dependent on the out-of-plane coordinate, z. This approach was chosen mainly because the conventional two-dimensional plane-strain approach cannot effectively represent the out-of-plane behavior of the skew reinforcement. Conversely, a truly three-dimensional analysis is prohibitively complicated and time consuming. The main advantage of the generalized plane-strain approach is that it can calculate the three-dimensional stresses and displacements while the finite-element grid remains in two dimensions.

The generalized plane-strain approach can calculate the approximate three-dimensional response of the system with minimal effort.

The total virtual work in the finite-element formulation is described as

$$\delta V = \sum_{e=1}^{N} \delta V_e$$

$$= \sum_{e=1}^{N} [\delta U_e - \delta W_e] = 0 \tag{1}$$

where

N = total number of elements,
δV_e = virtual work of element,
δU_e = element virtual internal energy, and
δW_e = element virtual external work.

The incremental material constitutive relationship is

$$\{\Delta\sigma\} = [C] \{\Delta\varepsilon\} \tag{2}$$

where

$\{\Delta\sigma\}$ = changes in stress vector,
$\{\Delta\varepsilon\}$ = changes in strain vector, and
$[C]$ = constitutive matrix.

Note that the constitutive matrix $[C]$ in incremental analysis depends on current stress state and its history. The element virtual internal energy expression can be written incrementally as

$$\delta\Delta U_e = \int_{V_e} \{\delta\varepsilon\}^T \{\Delta\sigma\} \, dV_e \tag{3}$$

where

$\delta \Delta U_e$ = incremental element virtual internal energy,
V_e = volume of the element, and
$\{\delta \varepsilon\}^T$ = incremental strain vector transpose.

Substitution of Equation 2 into Equation 3 yields

$$\delta \Delta U_e = \int_{V_e} \{\delta \varepsilon\}^T [C] \{\Delta \varepsilon\} \, dV_e \tag{4}$$

The three-dimensional displacements in generalized plane-strain approach are independent of the out-of-plane z coordinate; that is,

$$u = u(x, y)$$
$$v = v(x, y)$$
$$w = w(x, y) \tag{5}$$

From the definition of strains in three dimensions,

$$\{\varepsilon\} = \{\varepsilon_x, \varepsilon_y, \varepsilon_z, \gamma_{xy}, \gamma_{xz}, \gamma_{yz}\}^T$$

$$= \begin{bmatrix} \dfrac{\partial u}{\partial x} \\ \dfrac{\partial y}{\partial y} \\ \dfrac{\partial w}{\partial z} \\ \dfrac{\partial u}{\partial y} + \dfrac{\partial y}{\partial x} \\ \dfrac{\partial u}{\partial z} + \dfrac{\partial w}{\partial x} \\ \dfrac{\partial v}{\partial z} + \dfrac{\partial w}{\partial y} \end{bmatrix} \tag{6}$$

where ε equals normal strain and γ equals shear strain.

It is evident that the strain components in generalized plane strain are

$$\{\varepsilon\} = \begin{bmatrix} \dfrac{\partial u}{\partial x} \\ \dfrac{\partial v}{\partial y} \\ 0 \\ \dfrac{\partial u}{\partial y} + \dfrac{\partial v}{\partial x} \\ \dfrac{\partial w}{\partial x} \\ \dfrac{\partial w}{\partial y} \end{bmatrix} \tag{7}$$

By using a linear approximation for displacements, the three displacements at each node of the isoparametric quadrilateral continuum element can be approximated as

$$u = \sum_{i=1}^{4} N_i u_i$$

$$v = \sum_{i=1}^{4} N_i v_i$$

$$w = \sum_{i=1}^{4} N_i w_i \tag{8}$$

where u_i, v_i, w_i equals the approximate ith nodal displacements and N_i equals first-order shape function.

Substituting Equation 8 into Equation 7 yields

$$\varepsilon_x = \frac{\partial u}{\partial x}$$
$$= \frac{\partial}{\partial x} \left[\sum_{i=1}^{4} N_i u_i \right]$$
$$= \sum_{i=1}^{4} F_i u_i$$

$$\varepsilon_y = \frac{\partial v}{\partial y}$$
$$= \frac{\partial}{\partial y} \left[\sum_{i=1}^{4} N_i v_i \right]$$
$$= \sum_{i=1}^{4} G_i v_i$$

$$\gamma_{xy} = \frac{\partial u}{\partial y} + \frac{\partial y}{\partial x}$$
$$= \frac{\partial}{\partial y} \left[\sum_{i=1}^{4} N_i u_i \right] + \frac{\partial}{\partial x} \left[\sum_{i=1}^{4} N_i v_i \right]$$
$$= \sum_{i=1}^{4} \left[G_i u_i + F_i v_i \right]$$

$$\gamma_{xz} = \frac{\partial w}{\partial x}$$
$$= \sum_{i=1}^{4} F_i w_i$$

$$\gamma_{yz} = \frac{\partial w}{\partial y}$$
$$= \sum_{i=1}^{4} G_i w_i \tag{9}$$

where

$$F_i = \frac{\partial N_i}{\partial x}$$

$$G_i = \frac{\partial N_i}{\partial y}$$

The incremental strain-displacement relationships are

$$\{\Delta\varepsilon\}_e = [B]\{\Delta u\}_e \qquad (10)$$

where

$\{\Delta\varepsilon\}_e$ = element incremental strain vector,
$\{\Delta u\}_e$ = element incremental displacement vector
$= \{\Delta u_1, \Delta u_2, \Delta u_3, \Delta u_4, \Delta v_1, \Delta v_2, \Delta v_3, \Delta v_4, \Delta w_1, \Delta w_2, \Delta w_3, \Delta w_4\}^T$,

$$[B] = \begin{bmatrix} \{F\}^T & \{0\}^T & \{0\}^T \\ \{0\}^T & \{G\}^T & \{0\}^T \\ \{0\}^T & \{0\}^T & \{0\}^T \\ \{G\}^T & \{F\}^T & \{0\}^T \\ \{0\}^T & \{0\}^T & \{F\}^T \\ \{0\}^T & \{0\}^T & \{G\}^T \end{bmatrix} 6 \times 12,$$

$\{F\}^T = \{F_1, F_2, F_3, F_4\}$,
$\{G\}^T = \{G_1, G_2, G_3, G_4\}$, and
$\{0\}^T$ = null vector transpose.

Substitution of Equation 10 into Equation 4 yields

$$\delta\Delta U_e = \int_{V_e} \{[B]\{\delta u\}_e\}^T [C] \{[B]\{\Delta u\}_e\}\, dV_e$$

$$= \{\delta u\}_e^T [EK] \{\Delta u\}_e \qquad (11)$$

where

$[EK]$ = element tangent stiffness matrix with a dimension of 12×12
$= \int_{V_e} [B]^T [C] [B]\, dV_e$ and
$[C]$ = incremental constitutive matrix.

The coefficients of matrix $[C]$ can be obtained from the stress-strain relationship.

If a nonlinear soil characterization is used, then the soil tangent modulus depends on the current stress state and its history. Therefore, the correct value of soil tangent modulus and the matrices $[C]$ and $[EK]$ must be determined from an iteration process.

Once the element tangent stiffness matrices are determined for each element, they are assembled to obtain a global system stiffness matrix based on the element-node arrangement. Meanwhile, the element load vectors, resulting from gravity loading and traction, are assembled separately to produce a global system load vector. Finally, a set of simultaneous equations satisfying the boundary conditions is obtained and the equations are solved to obtain the global nodal displacements. The obtained nodal displacements are then used to calculate the strains and the stresses. The calculated stresses are used to estimate a set of new soil tangent modulus values for the next iteration when nonlinear soil properties are considered.

The special characteristics of the generalized plane-strain finite-element analysis must be reiterated. Conventional two-dimensional plane-strain finite-element analysis requires the size of element stiffness matrix, $[EK]$, to be 8×8 (i.e., two displacements along x and y coordinates at each of the four nodes of a linear isoparametric quadrilateral element). Conversely, truly three-dimensional finite-element analysis requires an element stiffness matrix $[EK]$ of 24×24 for a linear isoparametric brick element because three displacements exist at each of eight nodes. The generalized plane-strain finite-element analysis requires an element stiffness matrix $[EK]$ of 12×12 (i.e., three displacements at each of four nodes of a linear isoparametric quadrilateral element). A smaller element stiffness matrix is always desirable because the majority of the computational effort in finite-element analysis comes from the solution of simultaneous equations.

COMPARISON WITH THREE-DIMENSIONAL SOLUTIONS

A comparison has been made with the results obtained from a truly three-dimensional analysis (6) to illustrate the effectiveness of the generalized plane-strain finite-element method of analysis. Figure 1 presents a schematic description of the problem considered for the comparison and it includes an L-shaped bridge abutment reinforced with tie-rods and drilled-in concrete anchors. The tie-rods are made of steel with a yield strength of 90,000 lb/in.², a diameter of 1.5 in., and a skew angle of 11.31 degrees to the plane perpendicular to the abutment. The drilled-in concrete anchors are 2.5 ft in diameter with a length of 5 ft. The abutment stem and base have uniform thickness of 1 ft. It rests on top of linear elastic soil with Poisson's ratio of 0.3, tangent modulus of 3,500 lb/in.², and unit weight of 120 lb/ft³.

The tie-rods and drilled-in concrete anchors are simulated by the beam-column elements in both the generalized plane-
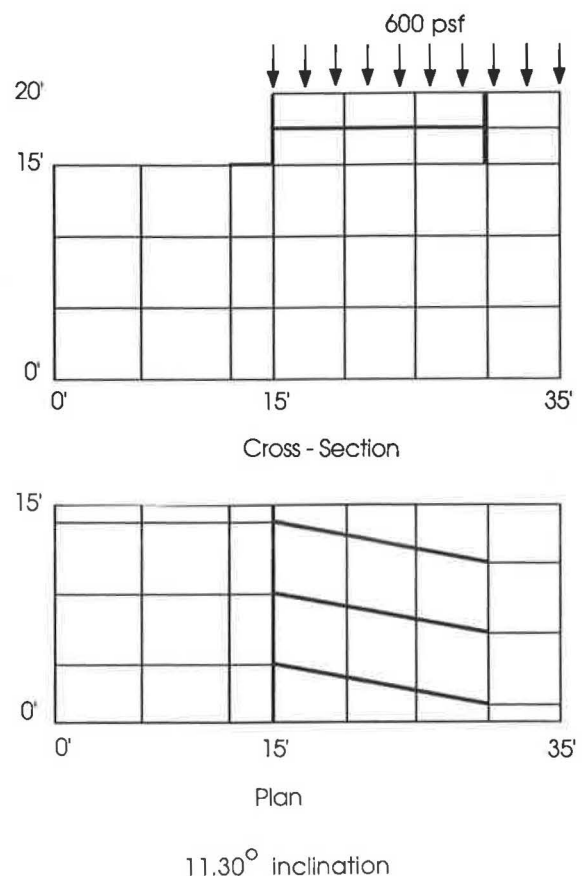

FIGURE 1 Schematics of tie-back wall.

strain and the truly three-dimensional finite-element analysis. The generalized plane-strain finite-element approach, by virtue of its two-dimensional finite-element grid, allows beam-column elements to model the abutment. However, plate elements are needed in the truly three-dimensional finite-element analysis (7).

A total of 42 nodes, 29 isoparametric quadrilateral continuum elements, and 8 beam-column elements are used in the generalized plane-strain finite-element analysis, whereas the three-dimensional analysis requires a total of 210 nodes, 116 brick elements to model the continuum, 9 beam-column elements for the tie-rods, 6 beam-column elements for the drilled-in concrete anchors, and 12 plate elements for the abutment. It required a CDC Cyber-180 mainframe computer approximately 8.5 and 182.5 sec of CPU time, to complete the generalized plane-strain finite-element analysis and the truly three-dimensional finite element analysis, respectively, resulting in a ratio of 21.5 in computational time.

Tables 1 and 2 present comparisons of three-dimensional displacements at selected nodes and the responses of the structural members. The differences are virtually negligible. Thus, the generalized plane-strain finite-element method of analysis can effectively capture most of the significant three-dimensional response of the skew retaining structures without significant error but with a remarkable reduction in computational effort.

EFFECT OF SKEW ANGLE

A Reinforced Earth retaining wall has been analyzed (8) to develop an understanding of the effect of skew angle. The wall has reinforcing strips installed horizontally with equal spacing and skew angle. The soil considered is silty sand with a friction angle of 32 degrees and no cohesion and is modeled by the nonlinear hyperbolic soil characterization proposed by Duncan et al. (9).
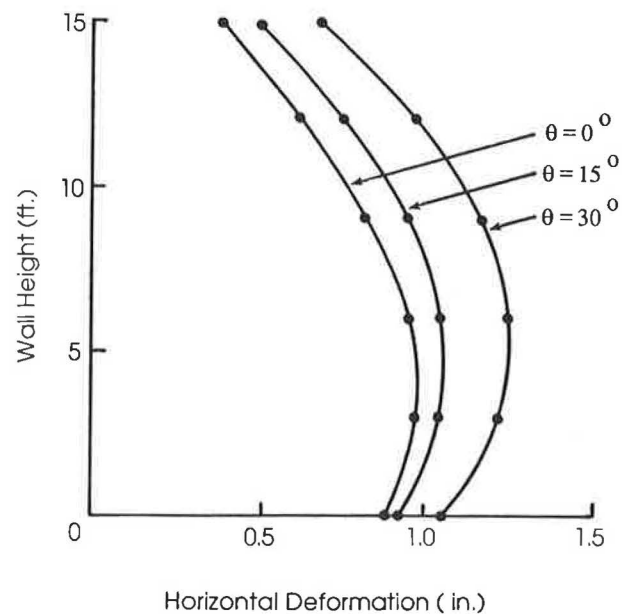

FIGURE 2 Horizontal deformation of Reinforced Earth wall.

The main variable considered in the study is the skew angle of the reinforcing strips, which varies from 0 to 30 degrees. The reinforcing members are made of metal strips 2.5 in. in width, ⅛ in. in thickness, 15 ft in length, and a spacing of 3 ft both horizontally and vertically. The height of the wall remains as 18 ft.

Figure 2 presents the calculated deformations of the retaining walls with different skew angles. As the skew angle increases, the larger outward movements result. For instance, maximum outward movement of 0.96 in. occurs with no skew angle, whereas 1.24 in. of maximum outward movement is expected with 30 degree skew angle, resulting in an increase of approximately 29 percent. However, the pattern of outward bulge

TABLE 1 COMPARISON OF DISPLACEMENTS AT NODES ALONG THE MIDDLE TIE-BACK

Nodal Distance from Abutment	u (ft.)		v (ft.)		w (ft.)	
	GPS	3-D	GPS	3-D	GPS	3-D
0 ft.	0.015	0.014	- 0.390	- 0.391	- 0.006	- 0.000
5 ft.	0.011	0.010	- 0.552	- 0.556	0.003	0.003
10 ft.	0.012	0.012	- 0.617	- 0.622	- 0.002	- 0.002
15 ft.	0.008	0.008	- 0.618	- 0.622	0.004	0.002

TABLE 2 COMPARISON OF FORCES AND MOMENTS

	Axial Force (lbs.)		Shear (lbs.)		Bending Moment (ft.-lbs.)	
	GPS	3-D	GPS	3-D	GPS	3-D
Concrete Anchor	12,360	11,030	977	952	29,243	28,544
Tie-Rod	390	401				

of the wall becomes slightly different as the skew angle increases. Maximum outward deformation occurs toward the toe of the wall when the skew angle is zero or relatively small, with a gradual upward shift as the skew angle increases. The out-of-plane directional displacements, as presented in Figure 3, indicate a similar pattern. As was expected, the out-of-plane displacements become larger as the skew angle increases. The conventional plane-strain approach is not capable of calculating this out-of-plane displacement directly.

The same formulation has been applied to analyze an L-shaped concrete bridge abutment reinforced with skew tie-backs (8). The abutment has dimensions of 8 ft in height and 1 ft in stem thickness with a 5-ft wide and 2.5-ft thick base and is supported by 40-ft-long and 1-ft-diameter friction timber piles, which are installed in two rows. The front row consists of one pile per group and the rear row of two piles per group. The spacings of the pile group and the tie-backs are both 12.73 ft. The external loads include a surcharge of
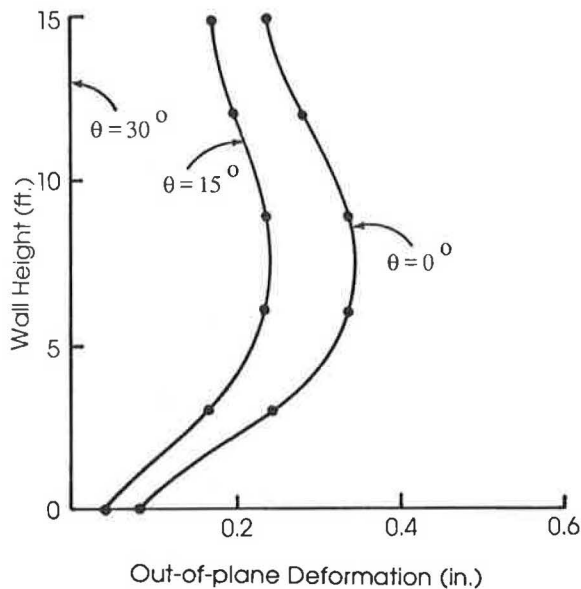
650 psf and a bridge girder support reaction of 6,800 lb/ft acting on the base of the abutment. The backfill material consists of crushed limestone, and the foundation soil consists of silty clay. The strength and the hyperbolic soil properties are presented in Table 3. The tie-rods have a diameter of $1\frac{3}{8}$ in. and a length of 35 ft and are embedded at a depth of 2.67 ft from the ground surface and are tied to 2.5 ft diameter drilled-in concrete anchors.

Figure 4 presents the variations of tie-rod axial force and abutment bending moment as a function of skew angle and indicates that the axial force within the tie-rod decreases as the skew angle increases. However, the pattern of bending moment developed within the abutment is the opposite. However, the rate of bending moment increase is very small. For instance, increasing the skew angle from zero degrees to 45 degrees results in an increase of bending moment of a mere 3.5 percent.

The out-of-plane displacement at the top of the abutment indicates an almost identical pattern to that of the Reinforced Earth wall, increasing rapidly from zero (with no skew angle) as the skew angle increases. However, the out-of-plane displacement remains more or less the same beyond a skew angle of approximately 30 degrees (Figure 5).
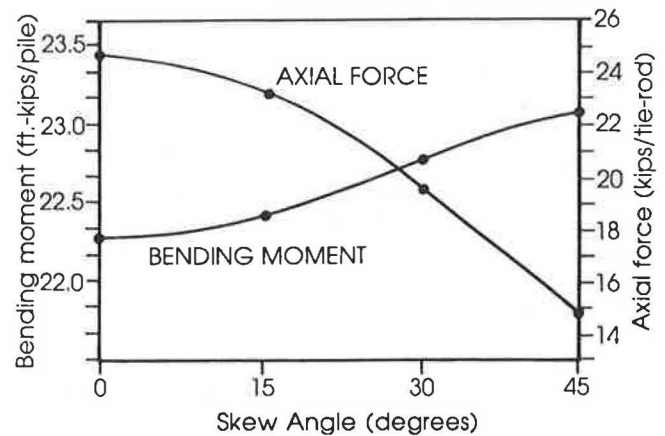

FIGURE 3   Out-of-plane deformation of Reinforced Earth wall.

FIGURE 4   Axial force and bending moment of tie-back wall.

TABLE 3 SOIL PARAMETERS

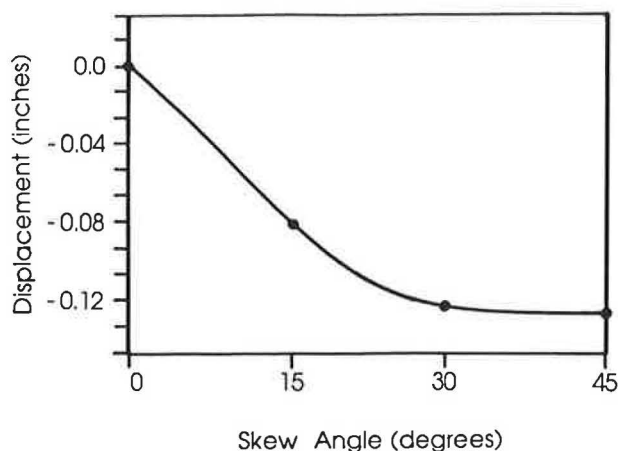|	Crushed Limestone	Silty Clay
Unit Weight (lb/ft^3)	103.5	136
Cohesion (psf)	0	1,100
Friction Angle (deg)	50	35
Loading Modulus	700	215
Modulus Exponent	0.85	0.41
Failure Ratio	0.74	0.60
Poisson's Ratio	0.3	0.3

FIGURE 5 Out-of-plane deformation of tie-back wall.

CONCLUSION

Development of a finite-element method of analysis based on the generalized plane-strain approach is briefly described and has been applied to compare the results with those obtained from a truly three-dimensional analysis. The comparison indicates that the generalized plane-strain method of analysis is very effective and efficient in calculating the three-dimensional response of earth-retaining structures with skew reinforcement without a significant loss in accuracy.

A study is also included of the effect of skew angle associated with retaining structures by using the generalized plane-strain method of analysis. Considered in the analysis are the Reinforced Earth retaining wall reinforced with skew metal strips and the conventional reinforced concrete abutment reinforced with skew tie-backs.

The generalized plane strain method of analysis is intended to capture the most essential characteristics involved in earth-retaining structures with skew reinforcement without resorting to a fully three-dimensional analysis. Though the study shows a promising capability of the developed method analysis, a more detailed study must be conducted to verify the validity of the formulation further.

REFERENCES

1. H. Vidal. The Principle of Reinforced Earth. In *Highway Research Record 282*, HRB, National Research Council, Washington, D.C., 1969.
2. J. K. Mitchell and W. C. B. Villet. *NCHRP Report 290: Reinforcement of Earth Slopes and Embankments*. TRB, National Research Council, Washington, D.C., June 1987.
3. C. K. Shen, S. Bang, and L. R. Herrmann. Ground Movement Analysis of Earth Support System. *Journal of the Geotechnical Engineering Division*, ASCE, GT12, Dec. 1981.
4. S. Bang. *Design and Analysis of Reinforcing Distressed Bridge Abutments*. Final Report, South Dakota Department of Transportation, Oct. 1988.
5. S. Bang and C. K. Shen. *Soil Reinforcement in Soft Ground Tunneling*. Report DOT/RSPA/DMA-50/83/15, U.S. Department of Transportation, Jan. 1983.
6. K. J. Bathe, E. L. Wilson, and F. E. Peterson. *SAPIV: A Structural Analysis Program for Static and Dynamic Response of Linear Systems*. Report EERC73-11, University of California, Berkeley, April 1974.
7. S. Bang and S. Schelske. Bridge Abutments Reinforced with Skew Tie-Backs. Presented at 3rd International Conference on Numerical Models in Geomechanics, Niagara Falls, Canada, May 1989.
8. S. Bang and S. I. Hwang. Analysis of Skew Reinforcement System. Presented at 24th Annual Engineering Geology and Soils Engineering Symposium, Coeur d'Alene, Idaho, March 1988.
9. J. M. Duncan, P. Byrne, K. S. Wong, and P. Mabry. *Strength, Stress-Strain and Bulk Modulus Parameters for Finite Element Analysis of Stresses and Movements in Soil Masses*. Report UBC/GT/80-01, Department of Civil Engineering, University of California, Berkeley, Aug. 1980.